Japanese Journal of Applied Physics

The Japan Society of Applied Physics

REGULAR PAPERS

Fabrication and energy harvesting characteristics of unimorph piezoelectric cantilever generators with interdigitated electrode lead zirconate titanate laminates

To cite this article: Min-seon Lee *et al* 2017 *Jpn. J. Appl. Phys.* **56** 127101

View the article online for updates and enhancements.

Related content

- Fabrication and characterization of free-standing thick-film piezoelectric cantilevers for energy harvesting
  Swee-Leong Kok, Neil M White and Nick R Harris
- Review Article
  S P Beeby, M J Tudor and N M White
- Fabrication and performance evaluation of a metal-based bimorph piezoelectric MEMS generator for vibration energy harvesting
  Chun-Liang Kuo, Shun-Chiu Lin and Wen-Jong Wu

This content was downloaded from IP address 131.215.225.9 on 17/11/2017 at 08:04

Japanese Journal of Applied Physics **56**, 127101 (2017)
https://doi.org/10.7567/JJAP.56.127101

REGULAR PAPER

Fabrication and energy harvesting characteristics of unimorph piezoelectric cantilever generators with interdigitated electrode lead zirconate titanate laminates

Min-seon Lee[1,2], Ji-sun Yun[1], Woon-ik Park[1], Youn-woo Hong[1], Jeong-ho Cho[1], Jong-hoo Paik[1], Yong Ho Park[2*], Chun-myung Son[3], and Young Hun Jeong[1*]

[1]*Electronic Convergence Materials Division, Korea Institute of Ceramic Engineering and Technology, Jinju, Gyeongnam 52851, Republic of Korea*
[2]*Department of Materials Science and Engineering, Pusan National University, Busan 46241, Republic of Korea*
[3]*KEPCO KDN Co., Ltd., Naju, Jeonnam 58322, Republic of Korea*

Received May 31, 2017; revised August 16, 2017; accepted September 10, 2017; published online November 16, 2017

Interdigitated electrode (IDE) unimorph piezoelectric cantilever generators (UPCGs) were fabricated and their energy harvesting characteristics were investigated. A hard lead zirconate titanate (PZT) material with a high mechanical quality factor (Q_m) of 1280 was used for the active piezoelectric film of the IDE UPCGs. Two different laminated IDE UPCGs were prepared; one has Ag/Pd interdigitated electrode (IDE) formed only on the top and bottom PZT sheets (D-IDE), while the other has Ag/Pd IDE on all of the PZT sheets (M-IDE). Cofiring was conducted at 1050 °C for 2 h for PZT laminates with IDEs. The fabricated IDE UPCGs exhibited power densities of 50.4 μW/cm^3 for the D-IDE and 820 μW/cm^3 for the M-IDE. The UPCG with the M-IDE exhibited a higher performance than that with the D-IDE. Specifically, a significantly enhanced normalized power factor of 670 μW/(g^2·cm^3) was found at 118 Hz across 100 kΩ. © 2017 The Japan Society of Applied Physics

1. Introduction

Over the last decade, research on piezoelectrics around the world has considerably targeted vibration energy harvesting as a potential alternative to batteries.[1–5] Piezoelectric energy harvesting is suitable for harnessing environmental vibrations and converting them into usable electrical energy. A piezoelectric ceramic film coated on a cantilever beam, known as a piezoelectric cantilever generator, allows effective vibration energy harvesting at a relatively low ambient frequency of around 10 to 200 Hz. In general, a unimorph piezoelectric cantilever generator (UPCG) is widely utilized owing to its simple structure in which only one piezoelectric layer is attached to an elastic substrate beam.[6–8]

One of the most important design parameters when designing a UPCG is the resonant frequency, as the electrical output power performance can be maximized when the vibration frequency matches its resonant counterpart. The figure of merit (FOM) for a piezoelectric material on a resonant UPCG correlates with the electromechanical coupling factor (k), mechanical quality factor (Q_m), and elastic compliance under a constant electric field (s^E), as shown by[9]

$$\mathrm{FOM}_{\text{on-resonance}} = \frac{k^2 \cdot Q_m}{s^E}. \quad (1)$$

Among these parameters, Q_m would be dominant, as it presents a significant difference, while the others are not significant for most commercial hard and soft lead zirconate titanate (PZT) ceramics. Therefore, it appears that a hard PZT ceramic, which has a much higher Q_m value than the soft type, is attractive for a higher harvesting performance in UPCGs driven at a specific resonant frequency. Another important design parameter of a UPCG is the vibration mode to enhance the performance of the output power. Typically, resonating UPCGs vibrate in the transverse or longitudinal bending mode (known as the 3-1 or 3-3 mode, respectively). In the transverse bending mode, voltage occurs as stress acts in the thickness direction when electrodes are attached to both surfaces of a piezoelectric film, whereas it appears as stress acts in the longitudinal direction (in-plane) perpendicular to the thickness direction in the longitudinal bending mode (Fig. 1).[10] Although the transverse mode is commonly

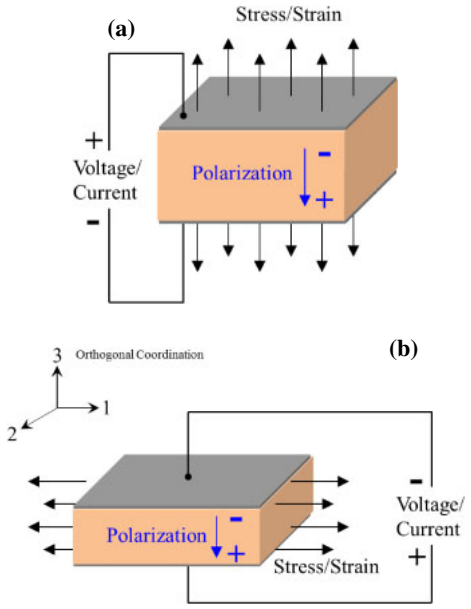

Fig. 1. (Color online) Schematics of the piezoelectric transduction modes: (a) longitudinal mode (3-3) and (b) transverse mode (3-1).

used for UPCGs,[11–13] a superior FOM can be implemented through the longitudinal mode because the longitudinal electromechanical coupling efficiency (k^2) can be 3–5 times higher than the transversal type.[14,15] Numerous piezoelectric thin film cantilever generators based on micro-electromechanical systems (MEMS) have been studied for energy harvesting applications.[16–21] Good power generation performance characteristics of these devices in the longitudinal vibration mode were demonstrated by applying an interdigitated electrode (IDE) pattern onto the piezoelectric film. Nevertheless, no studies to the best of the authors' knowledge have dealt with the fabrication and energy harvesting characteristics of an UPCG driven in the longitudinal vibration mode with a thick film fabrication process intended for commercialization.

Therefore, in this work, we fabricated a piezoelectric PZT ($Q_m = 1280$) thick film using a conventional tape casting process. Subsequently, a laminate structure composed of ten

© 2017 The Japan Society of Applied Physics

Table I. Piezoelectric properties of a sintered ceramic disk using commercial PZT-based piezoelectric powders (MPT) produced from Hayashi Chemicals.

Sintering temperature (°C)	1050
Curie temperature T_c (°C)	290
Coupling coefficient k_{33} (%)	61.1
Mechanical quality factor (Q_m)	
PZT	1280
Unimorph cantilever	1098
Piezoelectric charge constant d_{33} (C/N)	306×10^{-12}
Piezoelectric voltage constant g_{33} (V·m/N)	25×10^{-3}
Elastic compliance s_{33}^E (m^2/N)	20.2×10^{-12}
Dielectric constant $\varepsilon_{33}^T/\varepsilon_0$	1398
Dissipation factor (%)	0.6

Table II. Detailed dimensions of the hard PZT unimorph PCG with IDE fabricated in this work in mm.

Length of steel substrate (l_s)	52
Width of steel substrate (w_s)	16
Thickness of steel substrate (t_s)	0.3
Length of PZT laminate (l_p)	43.9
Width of PZT laminate (w_p)	13.6
Thickness of PZT laminate (t_p)	0.28
Length of overall IDE (l_{ide})	43.06
Width of overall IDE (w_{ide})	12.85
Thickness of overall IDE (t_{ide})	0.002
Length of IDE finger (l_{ef})	11.57
Width of IDE finger (w_{ef})	0.075
Gap between adjacent IDE fingers (s_{ef})	0.436

PZT sheets with double and multiple-layer IDEs was developed to use these layers as the active layer in a UPCG driven in the longitudinal vibration mode. The energy harvesting characteristics of these samples were comparatively evaluated as a function of the frequency and resistive load with a view towards vibration energy harvester applications.

2. Experimental procedure

PZT-based commercial piezoelectric powders (Hayashi Chemicals MPT) were prepared to obtain green sheets by a conventional tape casting process. PZT powders have good dielectric and hard piezoelectric properties with a high Q_m of 1280, as shown in Table I. To formulate a viscous casting slurry, toluene (Samchun Pure Chemical), ethanol (Samchun Pure Chemical), and poly(vinyl butyral) (Sekisui BM-SZ) were added to the PZT powders. Dibutylphthalate (Daejung Chemical & Metals) and a dispersant (BYK-Chemie BYK-111) were also added and mixed with the PZT powders at an optimum ratio. Subsequently, the mixed slurry was injected into a polyethylene bottle and remixed and then pulverized for 24 h using zirconia balls as media. The mixed slurry was then uniformly sieved using a screen consisting of a mesh structure, with the air bubbles in the slurry sufficiently removed after 1 h in a −760 mmHg vacuum using a vacuum deaerator. A uniform PZT green sheet with a thickness of about 35 μm was produced and rolled up using a tape casting machine with a doctor blade (Techgen TCA-2000). To print the IDE pattern onto the surface of a tailored ($15 \times 20\,cm^2$) PZT green sheet, a screen mask (Sejinsmark) was designed and prepared with the dimensions ($12.85 \times 43.06\,mm^2$) of the overall IDE pattern. Details of the designed IDE configuration can be found in Table II. A Ag–Pd (30% Pd incorporated Winner Technology WT-SPD30-A) IDE was successfully printed onto the PZT green sheet. Generally, 20 PZT green sheets were prepared to obtain two PZT laminates with IDEs. The first is a PZT laminate with a double-layer IDE, where the IDE print generally lies only on the top and bottom layers of 10 PZT layers (D-IDE), and a PZT laminate with a multilayer IDE for which all ten PZT layers have the IDE print on the top surface in each case (M-IDE). Thereafter, they were laminated under 13 MPa, at a temperature of 60 °C using a laminator (Keko), after which they underwent warm isostatic pressing (WIP) at 250 bar and a temperature of 65 °C for 20 min. The two manufactured PZT laminates were successfully cofired at 1050 °C for 2 h.

To fabricate a U PCG, a cofired PZT laminate with an IDE was bonded on the top surface of a commercially available 300-μm-thick substrate (t_s) made of carbon-incorporated steel using an epoxy adhesive. The elastic steel substrate was used 16 mm (width; w_s) × 52 mm (length; l_s) in size. One end of the elastic substrate was clamped to a rigid wall and the other end was free without any proof mass.

Field-effect scanning electron microscopy (FE-SEM; JEOL JSM-7610F) was performed to observe the microstructure of the PZT laminates with IDEs. The ferroelectric polarization to electric field (P–E) hysteresis was also observed using a ferroelectric test system (Radiant technology RT66A). To evaluate the energy harvesting characteristics of the U PCG for the PZT laminates with IDEs, a shaker (Brüel & Kjær 4809) with a high-speed bipolar amplifier (NF HSA4014) was utilized. The amplifier was driven by a functional generator (Agilent 33220A), and the shaker provided periodic excitation with a harmonic signal. During the excitation acceleration step, the PCG and an accelerometer (ACO 3116) were placed on top of the shaker. The harmonic vibration frequency was then varied from 10 to 150 Hz. The open-circuit voltages generated by unimorph PCGs were measured with an amplifier (LeCroy Wavejet 322).

3. Results and discussion

Figure 2(a) shows a schematic surface image of the IDE configuration patterned on a piezoelectric film. The IDE structure is commonly used to produce the poling axis of a piezoelectric material parallel to the in-plane direction, as shown in Fig. 2(b). It consists of two interlocking electrode combs with two long strips placed horizontally at both ends of a piezoelectric film substrate and with numerous electrode fingers in interdigitated form attached to these strips. An actual top-view image of the PZT laminate with an IDE cofired at 1050 °C for 2 h in this work is shown in Fig. 3. The overall IDE configuration can be shown as two more brightly colored comb shapes facing each other. There are 83 IDE fingers in total with 42 and 41 IDE fingers for the top and bottom combs, respectively. The PZT laminate was clearly flat in both the longitudinal and thickness directions, but significantly shortened in the length direction. A surface optical microscopy image, shown as the enlarged image denoted with the red arrow in Fig. 3, exhibits a local area near the IDE strip of the PZT laminate with a Ag/Pd IDE cofired at 1050 °C for 2 h. It was found that each IDE finger

© 2017 The Japan Society of Applied Physics

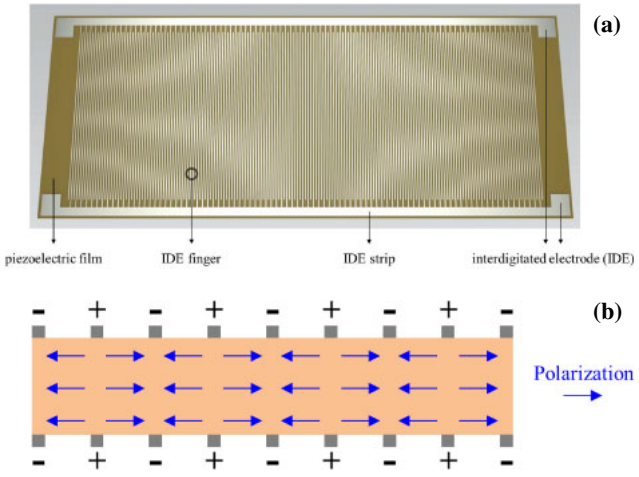

Fig. 2. (Color online) Schematic (a) surface image of the IDE configuration patterned on piezoelectric film and (b) cross-sectional image exhibiting polarization direction parallel to the in-plane direction.

was straight and that the IDE strip was well connected to each IDE finger. Moreover, no diffused trace of the Ag/Pd element was observed in this area. This also indicates that the electrode compound of Ag/Pd as used here is suitable for the cofiring of the hard PZT green laminate. A good surface morphology was similarly observed in all surface areas of the fabricated specimen. Detailed dimensions of the fabricated PZT laminate with an IDE are also presented in Table II. A considerably reduced gap (s_{ef}) of 436 μm and a width (w_{ef}) of 75 μm for the IDE configuration reveal that the sintered PZT laminate was sufficiently densified and crystallized after sintering at 1050 °C, referring to the designed IDE configuration with s_{ef} (500 μm) and w_{ef} (100 μm) prior to sintering.

Figures 4(a) and 4(b) show cross-sectional FE-SEM images of the PZT laminates with the D-IDE and M-IDE, respectively, cofired at 1050 °C for 2 h. A thickness of approximately 280 μm and a highly dense microstructure were commonly obtained for both specimens. Parallel IDE fingers denoted by white arrows on the top surface of the specimen with the D-IDE are clearly observed (not in the case, however, with the M-IDE owing to dust and ash formed during the muffled sintering process). The IDE fingers embedded in the PZT laminate were also examined, as indicated by the white dotted rectangle. It was found that the cofiring process was successful considering that no voids or instances of delamination were observed in the PZT laminate. However, the vertically aligned IDE fingers formed a meandering array for the specimen with the M-IDE, possibly owing to an experimental error during the lamination step, as shown in Fig. 4(b) (related to the fact that this is not a simple process).

A *P*–*E* hysteresis loop obtained from the PZT laminate with an IDE is shown in Fig. 5. Prior to the *P*–*E* measurement, a poling process was conducted by applying an electric field of 2.2 kV/mm at 100 °C for 10 min in an oil bath in order to fully orient the ferroelectric domains along the plane direction. The specimen with the D-IDE shows a normal hysteresis loop, but the specimen with the M-IDE shows a propeller-type hysteresis loop, which may have arisen from the domain wall pinning caused by defects such as oxygen vacancies or antiferroelectricity with 180° domains stemming from the local longitudinal shift of the IDE finger array. However, additional investigations are needed to clarify this. The remnant polarization (P_r in C/cm^2) can be calculated from the induced charge (Q) as[22)]

$$P_r = \frac{Q}{l_{ef} \cdot t_p \cdot (N-1)}, \tag{2}$$

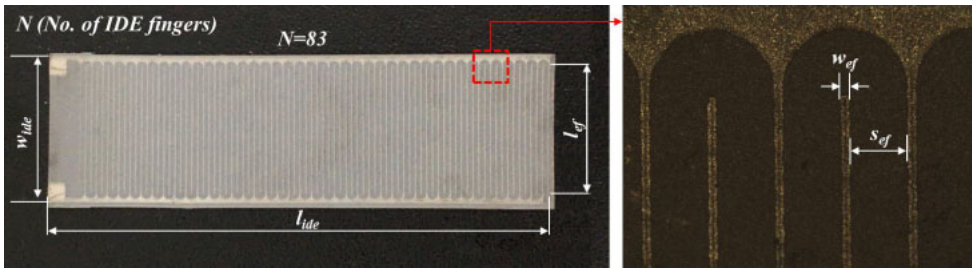

Fig. 3. (Color online) Actual image of the fabricated hard PZT laminate with IDE cofired at 1050 °C for 2 h (left) and enlarged image of the local area near the top IDE strip, denoted by the red dashed square (right).

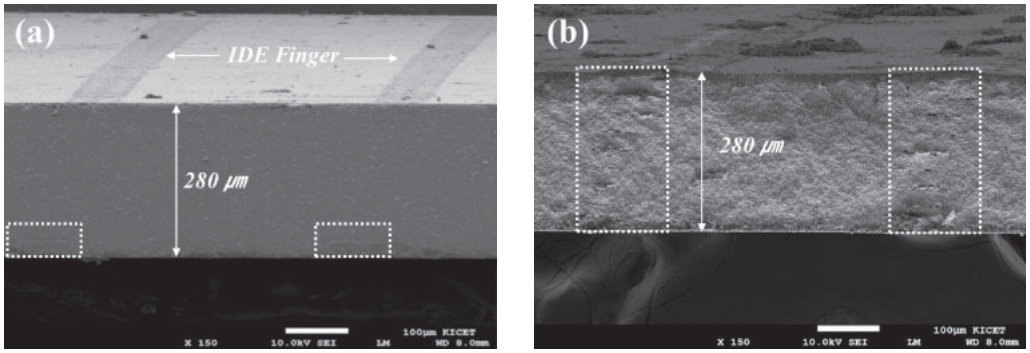

Fig. 4. Cross-sectional FE-SEM images of the hard PZT laminates with the (a) D-IDE and (b) M-IDE cofired at 1050 °C for 2 h.

© 2017 The Japan Society of Applied Physics

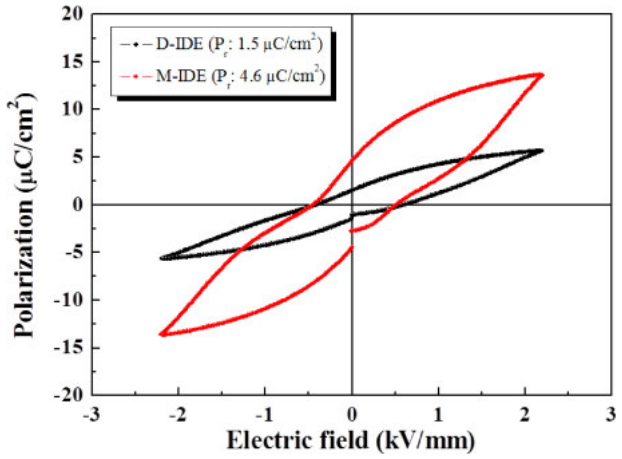

Fig. 5. (Color online) *P–E* hysteresis loops of the hard PZT laminates with the D-IDE and M-IDE.

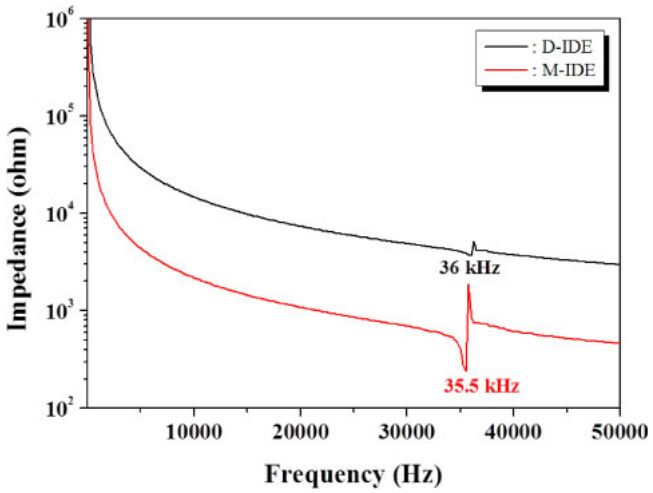

Fig. 6. (Color online) Impedance variations for the hard PZT laminates with the D-IDE and M-IDE as a function of frequency.

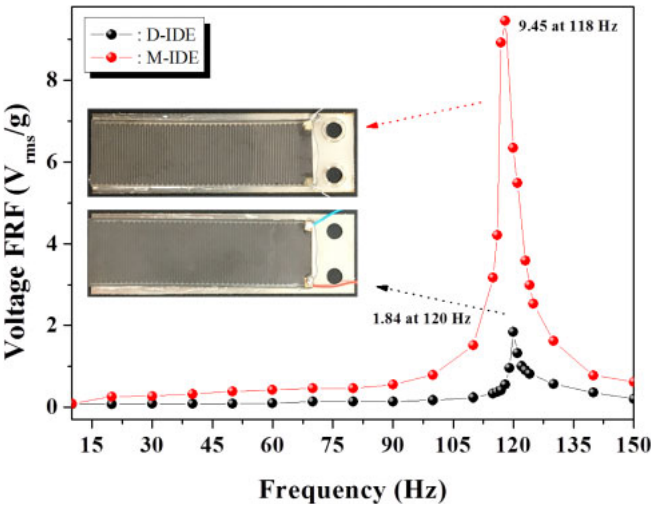

Fig. 7. (Color online) Frequency response functions of the output voltage for hard PZT U PCGs with the D-IDE and M-IDE (Inset images exhibit the two corresponding unimorph PCGs).

where l_{ef} is the length of the IDE finger, t_p is the thickness of the PZT laminate, and N is the total number of IDE fingers. It is clear that the P_r (4.6 μC/cm^2) of the PZT laminate with the M-IDE significantly inceased compared with that of the PZT laminate with the D-IDE, being almost three times higher. This is presumably due to the decreased inactive area (i.e., consisting of transition and dead areas) underneath the IDE fingers, which could not contribute to the total amount of induced charge because the polarization direction was not parallel to the in-plane direction.[23–25] The volume of the inactively polarized area inside the PZT laminate with the M-IDE can be reduced markedly by embedding more IDEs. Under the assumption that the applied electric field is uniform across the IDE finger gap, it can be predicted that a much higher P_r will be revealed for the PZT laminate. This effect can also be confirmed with the frequency-dependent impedance variation of the PZT laminate, as shown in Fig. 6. The measured frequency ranged from 20 Hz to 50 kHz. A markedly decreased impedance was observed for the M-IDE over the measured frequencies. As the PZT laminate fabricated with an IDE is a type of multilayer ceramic capacitor, its capacitance can be strongly enforced by the addition of additional IDE layers to the PZT laminate, resulting in a decrease in impedance (particularly the capacitive impedance). Resonance occurred at 35.5 and 36 kHz for the M-IDE and D-IDE samples, respectively. The capacitance of the resonant frequency was determined from the impedance plot in Fig. 6 to be 1.2 and 18.8 nF for the D-IDE and M-IDE, respectively. The decrease in the resonance frequency of the PZT laminate with the M-IDE was observed to be not significant. One end of the U PCG using the fabricated PZT laminate was tightly clamped onto a rigid supporting jig, resulting in a resonance frequency that markedly decreased to approximately 120 Hz.

Figure 7 shows the frequency response functions (FRFs) of the output voltage for the hard PZT U PCGs with the D-IDE and M-IDE, respectively. The frequency applied to a vibrator ranged from 10 to 150 Hz. This low frequency range could sufficiently reveal the resonance frequencies of the two devices under test (DUTs), considering the occurrence of electromechanical bending resonance due to the asymmetry of the PZT ceramic and the metallic steel beam. A very sharp peak was observed for both DUTs. The two peaks at 120 and 118 Hz correspond to the bending resonance frequencies of the U PCGs with the D-IDE and M-IDE, respectively, as indicated in the insets in images of Fig. 7. The sharp resonance peaks with a narrow operation frequency bandwidth were generated using the hard PZT piezoelectric ceramic with a high Q_m of 1280. The full width at half maximum at this frequency was less than 10 Hz for the DUTs. This strong frequency dependence can be limited for use in various vibration energy harvester applications demanding a wider frequency band range. However, the energy harvesting performance would be much higher when only operated at certain frequencies upon resonance. In this work, the hard PZT unimorph PCG with the M-IDE shows a high voltage FRF (9.45 V/g) at 118 Hz. At the beginning of this work, we intentionally designed the target resonance frequency of the unimorph PCG as 120 Hz (the second overtone of 60 Hz) to be used for self-powered health monitoring applications to industrial machines such as electrical motors operating at a fundamental frequency of 60 Hz. Frequency matching was fairly successfully achieved for the DUT with the D-IDE, but the process was inaccurate for the DUT with

© 2017 The Japan Society of Applied Physics

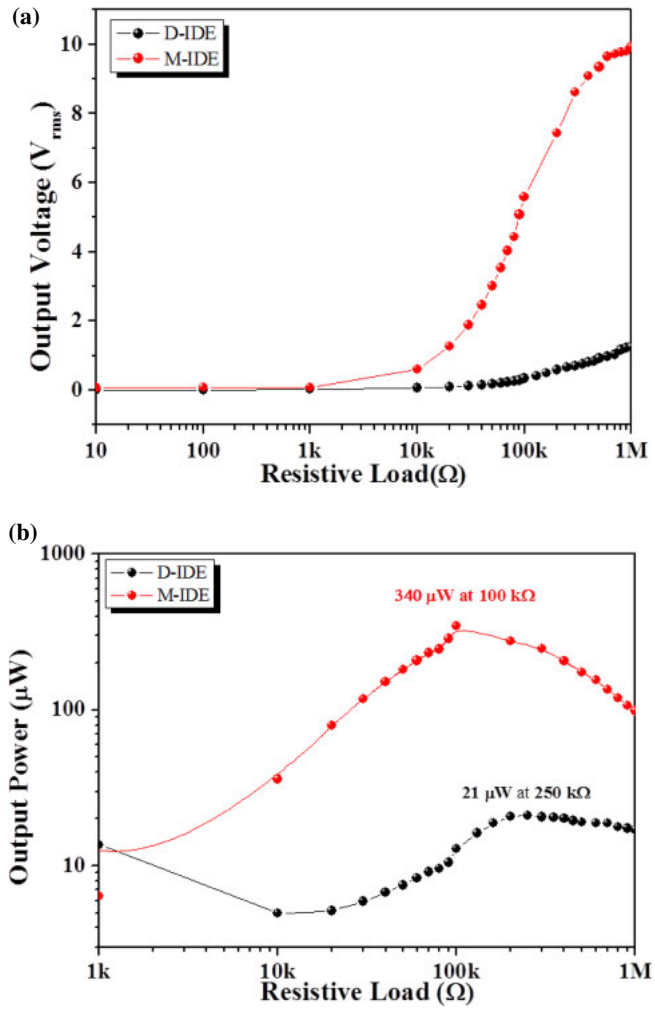

Fig. 8. (Color online) (a) Output voltage and (b) generated power varitations for hard PZT U PCGs with the D-IDE and M-IDE as a function of the resistive load.

the M-IDE. A slight modification (e.g., a volume reduction) to shift the frequency higher is required for operation upon resonance at 120 Hz.

Figure 8 shows output voltage and generated power variations for the PZT U PCGs with the D-IDE and M-IDE as a function of the resistive load at input accelerations of 1*g*. Increasing the load resistance to a maximum of 1 MΩ could increase the output voltage of the two DUTs. The increasing trend of the generated voltage was especially notable in the DUT with the M-IDE. The highest output power of 340 μW with a resistive load of 100 kΩ was also obtained for the same DUT upon resonance at 118 Hz. The generated power output characteristics in consideration of the global volume (PZT laminate and steel substrate) in this case correspond to a power density of 820 μW/cm^3 and a normalized power factor of 670 μW/(g^2·cm^3). The generalized electromechanical coupling factor (GEMC), an important parameter when attempting to determine the output power of PZT U PCGs, is also obtained from

$$K^2 = \frac{\omega_{\text{open}}^2 - \omega_{\text{short}}^2}{\omega_{\text{short}}^2}, \tag{3}$$

where ω_{short} and ω_{open} are the resonance angular frequencies of the associated short and open circuits, respectively.[26)]

Table III. Comparison of the energy harvesting characteristics upon resonance of two unimorph PZT laminates with the (a) D-IDE and (b) M-IDE.

Characteristics	(a)	(b)
Resonance frequency (Hz)	120	118
Output voltage (V_{rms})	4.3	10.4
Output power (μW)	21	340
Power density (μW/cm^3)	50.4	820
Power factor (μW/g^2)	1.7	280
Normalized power factor [μW/(g^2·cm^3)]	4.1	670
Generalized electromechanical coupling factor	1.73×10^{-3}	2.44×10^{-3}

According to Eq. (3), GEMCs of 1.73×10^{-3} (D-IDE) and 2.44×10^{-3} (M-IDE) were found according to the difference in resonant frequency between the low (10 Ω) and high (1 MΩ) load resistances. The energy harvesting characteristics of the two DUTs with the D-IDE and M-IDE are summarized in Table III.

4. Conclusions

In this work, two UPCGs, one with the D-IDE and the other with the M-IDE, were successfully developed and their energy harvesting characteristics were comparatively estimated as a function of the frequency and resistive load for vibration energy harvesting applications. During the preparation of piezoelectric film samples as an active layer in resonating UPCGs, a hard lead zirconate titanate (PZT) material with a high Q_m of 1280 was fabricated in the form of a 35-μm-thick ceramic sheet by a conventional tape casting method. Subsequently, a PZT laminate composed of ten sheets was prepared in two different forms, one (D-IDE) with a Ag/Pd IDE pattern formed only on the top and bottom PZT sheets, and the other (M-IDE) with an IDE on all PZT sheets. The laminated PZT films with the Ag/Pd IDE were successfully cofired at 1050 °C for 2 h. Consequently, highly dense PZT laminates could be obtained after sintering. It was observed that the P_r (4.6 μC/cm^2) of the PZT laminate with the M-IDE significantly increased compared with that of the PZT laminate with the D-IDE owing to the reduction in the inactively polarized area. Subsequently, two UPCGs, one using the PZT laminate with the D-IDE and the other with the M-IDE, were fabricated and their estimated energy harvesting characteristics were compared upon resonance under various resistive loads. The UPCG with the M-IDE exhibited a much higher performance than that with the D-IDE, with a high output voltage of 9.45 V under 1*g*, and it generated a power of 340 μW at 118 Hz across 100 kΩ, corresponding to a normalized power factor of 670 μW/(g^2·cm^3). These results imply that the energy harvesting performance capabilities of PCGs in the longitudinal mode can be enhanced further by embedding additional IDE layers in the PZT laminate.

Acknowledgment

This work was financially supported by the New and Renewable Energy Technology Development Program of the Korea Institute of Energy Technology Evaluation and Planning (KETEP, Nos. 20151120100260 and 20152020104960) through a grant funded by the Ministry of Trade, Industry and Energy of the Korean Government.

© 2017 The Japan Society of Applied Physics

1) E. S. Leland and P. K. Wright, Smart Mater. Struct. **15**, 1413 (2006).
2) A. Erturk and D. J. Inman, J. Intell. Mater. Syst. Struct. **19**, 1311 (2008).
3) N. E. Dutoit, B. L. Wardle, and S.-G. Kim, Integr. Ferroelectr. **71**, 121 (2005).
4) B. Edwards, P. A. Hu, and K. C. Aw, Smart Mater. Struct. **25**, 055019 (2016).
5) S. Du, Y. Jia, and A. A. Seshia, J. Intell. Mater. Syst. Struct. **28**, 1905 (2017).
6) J. W. Yi, W. Y. Shih, and W.-H. Shih, J. Appl. Phys. **91**, 1680 (2002).
7) X. Gao, W.-H. Shih, and W. Y. Shih, Appl. Phys. Lett. **97**, 233503 (2010).
8) O. Bilgen, M. A. Karami, D. J. Inman, and M. I. Friswell, Smart Mater. Struct. **20**, 055024 (2011).
9) V. Bedekar, J. Oliver, and S. Priya, IEEE Trans. Ultrason. Ferroelectr. Freq. Control **57**, 1513 (2010).
10) Q. Q. Zhang, S. J. Gross, S. Tadigadapa, T. N. Jackson, F. T. Djuth, and S. Trolier-McKinstry, Sens. Actuators A **105**, 91 (2003).
11) M.-A. Dubois and P. Muralt, Sens. Actuators A **77**, 106 (1999).
12) M. S. Bhuyan, S. H. M. Ali, M. Othman, B. Y. Majlis, S. A. Wahab, and S. Islam, Res. J. Appl. Sci. **9**, 86 (2014).
13) D. L. DeVoe and A. P. Pisano, J. Microelectromech. Syst. **6**, 266 (1997).
14) M. Colin, Q. Mortier, S. Basrour, and N. Bencheikh, J. Phys.: Conf. Ser. **476**, 012135 (2013).
15) T.-B. Xu, E. J. Siochi, J. H. Kang, L. Zuo, W. Zhou, X. Tang, and X. Jiang, Smart Mater. Struct. **22**, 065015 (2013).
16) Y. B. Jeon, R. Sood, J. H. Jeong, and S. G. Kim, Sens. Actuators A **122**, 16 (2005).
17) S. Saadon and O. Sidek, Energy Convers. Manage. **52**, 500 (2011).
18) H.-B. Fang, J.-Q. Liu, Z.-Y. Xu, L. Dong, L. Wang, D. Chen, B.-C. Cai, and Y. Liu, Microelectron. J. **37**, 1280 (2006).
19) J.-Q. Liu, H.-B. Fang, Z.-Y. Xu, X.-H. Mao, X.-C. Shen, D. Chen, H. Liao, and B.-C. Cai, Microelectron. J. **39**, 802 (2008).
20) G. Tang, B. Yang, C. Hou, G. Li, J. Liu, X. Chen, and C. Yang, Sci. Rep. **6**, 38798 (2016).
21) C.-L. Kuo, S.-C. Lin, and W.-J. Wu, Smart Mater. Struct. **25**, 105016 (2016).
22) B. Xu, R. G. Polcawich, S. Trolier-McKinstry, Y. Te, L. E. Cross, J. J. Bernstein, and R. Miller, Appl. Phys. Lett. **75**, 4180 (1999).
23) W. Beckert and W. S. Kreher, Comput. Mater. Sci. **26**, 36 (2003).
24) B. B. Nielsen, M. S. Nielsen, and I. F. Santos, J. Intell. Mater. Syst. Struct. **28**, 78 (2017).
25) R. R. Knight, C. Mo, and W. W. Clark, J. Electroceram. **26**, 14 (2011).
26) I. Kanno, T. Ichida, K. Adachi, H. Kotera, and K. Shibata, Sens. Actuators A **179**, 132 (2012).

© 2017 The Japan Society of Applied Physics